Journal of Nuclear Materials 389 (2009) 197–202

Contents lists available at ScienceDirect

Journal of Nuclear Materials

journal homepage: www.elsevier.com/locate/jnucmat

Dynamic observations of heavy-ion damage in Fe and Fe–Cr alloys

M.L. Jenkins [a,*], Z. Yao [a], M. Hernández-Mayoral [b], M.A. Kirk [c]

[a] Department of Materials, University of Oxford, Parks Rd., Oxford, OX1 3PH, UK
[b] Division of Materials, CIEMAT, Avenida Complutense 22, 28040-Madrid, Spain
[c] Material Science Division, Argonne National Laboratory, Argonne, IL 60439, USA

A B S T R A C T

We give an overview and summary of recent *in-situ* heavy-ion irradiation experiments on Fe and Fe–Cr alloys carried out on the Argonne IVEM Facility at irradiation temperatures up to 500 °C. Several new and unexpected observations were made. At low doses the contrast of new irradiation-induced dislocation loops sometimes developed over time intervals as long as 0.2 s, many orders of magnitude longer than expected for a process of cascade collapse. In addition at temperatures ⩽300 °C, "hopping" of 1/2<1 1 1> loops was induced by the ion or electron beams, especially in UHP Fe. At high doses complex microstructures developed in all materials, involving the formation of large interstitial loops. At 300 °C and RT these loops had Burgers vectors of type **b** = 1/2<1 1 1> and large shear components. At 500 °C only edge loops with **b** = <1 0 0> were produced.

1. Introduction

Candidate materials for structural applications in future fusion and advanced fission reactors include reduced-activation ferritic-martensitic (RAFM) steels with Cr contents ranging between 9% and 12%, such as EUROFER 97. These steels have better thermal properties and higher swelling resistance than austenitic steels, but may become embrittled under irradiation at temperatures less than about 400 °C [1–3]. In order to optimise RAFM steels for operation in a severe irradiation environment it is desirable to develop a detailed mechanistic understanding of the development of radiation damage in ferritic alloys, which is lacking at present. The work reported here is part of this endeavor. We have carried our *in-situ* irradiation experiments to observe dynamically in the transmission electron microscope (TEM) the development of radiation damage in pure Fe and Fe–Cr binary alloys with up to 18%Cr. These experiments were designed to yield data on the structure and properties of nano-scale defects generated by irradiation of simple model ferritic materials, and to underpin multi-scale modeling activities carried out at Oxford and elsewhere.

In the present paper we give a summary of the main results yielded by our work. Full details of the experiments carried out at room temperature (RT) and 300 °C has been published elsewhere [4,5]. We show here the first results of experiments carried out at irradiation temperatures of 500 °C, when completely different microstructures evolved at high doses compared with irradiations at lower temperatures.

2. Experimental details

The materials investigated included ultra-high purity, UHP Fe (containing ~1 ppm C, <5 ppm N, <10 ppm Si and very small quantities of other impurities) and Fe–Cr alloys (0–18 wt%Cr, of 99.99% purity). The cold-rolled as-received materials were annealed in vacuum at 800 °C for an hour followed by slow cooling. After this treatment all specimens had a simple ferritic microstructure with a low dislocation density. There was no evidence of any precipitation.

Thin foils were prepared by electropolishing and irradiated with 100–150 keV Fe^+ and Xe^+ ions at room temperature (RT) and at 300 °C and 500 °C in the Argonne IVEM-Tandem Facility [6]. The microscope was operated at 200 keV, below the threshold for knock-on damage in Fe. Dynamic TEM observations followed the evolution of damage over doses $\leqslant 2 \times 10^{19}$ ions m^{-2} (~13 dpa, according to a SRIM calculation with displacement energy 24 eV [7]). Irradiations were paused from time to time to allow detailed characterization of microstructures using a number of diffraction-contrast techniques (see [8]). Similar detailed characterization was performed at the end of the irradiation after specimens irradiated at elevated temperatures had cooled to RT.

3. Summary of results and discussion

3.1. Damage evolution at low doses

Small 2–4 nm dislocation loops first appeared at doses of about 10^{16} and 10^{17} ions m^{-2} depending on material and irradiation conditions. Fig. 1 shows typical microstructures at doses of the order of 5×10^{17} ions m^{-2} (about 0.3 dpa) in pure Fe and a range of

* Corresponding author. Tel.: +44 1865 273655; fax: +44 1865 283333.
E-mail address: mike.jenkins@materials.ox.ac.uk (M.L. Jenkins).

0022-3115/$ - see front matter © 2009 Elsevier B.V. All rights reserved.
doi:10.1016/j.jnucmat.2009.02.003

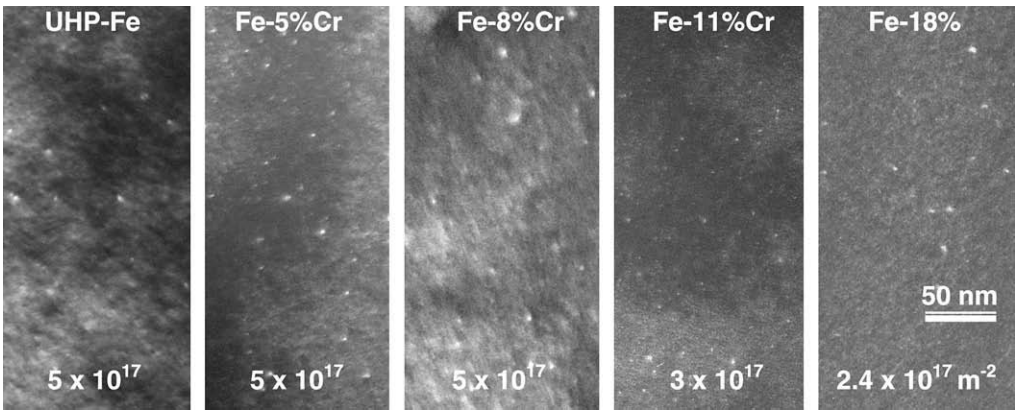

Fig. 1. Small dislocation loops in UHP Fe and in various Fe–Cr alloys at a relatively early stage of irradiation. In all cases except UHP Fe which was irradiated with 150 keV Fe^+ ions, the specimens were irradiated with 100 keV Fe^+ ions at room temperature. All are weak-beam images taken with **g** = 110, except Fe–18%Cr where **g** = 200, with doses as shown.

Fe–Cr alloys irradiated with Fe^+ ions at RT. In all cases dislocation loops are visible as small white dots. Similar result has been found previously in heavy-ion irradiations of pure Fe [9]. The threshold doses are much higher than in many other materials. Since substantial cascade overlap occurs at doses greater than about 10^{16} ions m^{-2}, this result suggests that loops are not generally formed by the collapse of individual cascades.

Contrast experiments carried out in <100> foils [4] showed that prismatic dislocation loops with Burgers vectors **b** = 1/2<111> and **b** = <100> were present at irradiation temperatures of 300 °C and RT. Loops with **b** = <100> were in a majority at lower doses. There was also a tendency for a higher proportion of <100> loops in pure Fe than in Fe–Cr alloys. These effects have not yet been fully quantified. We note that post-irradiation loop populations are very likely skewed by the loss of glissile 1/2<111> loops to the surface, as seen in the dynamic experiments reported below. In irradiations at 500 °C only <100> loops were found.

It was not possible to determine the vacancy or interstitial nature of loops directly. However, *ex-situ* experiments carried out on specimens irradiated with 30 keV Ga^+ ions at RT suggested that at least some of the loops are of vacancy character [4]. Vacancy loops have been found in many previous heavy-ion experiments, including experiments in Fe (e.g. [10]). Other observations (see below) suggest that interstitial loops may also be present, at least in thicker areas of foil at higher doses.

3.2. Dynamic observations at lower doses

In irradiations at 300 °C and RT, loops in all materials appeared in videos suddenly but often not instantaneously and then did not grow at doses less than about of 2×10^{18} ions m^{-2} (~1 dpa). The contrast of new loops sometimes developed over time intervals as long as 0.2 s, especially when produced by Xe^+ ions, although the same effect was also seen for Fe^+ ions [2]. An example of image intensity measurements made over several successive video frames is shown in Fig. 2. In this case, the contrast of a loop produced in Fe–8%Cr during 150 keV Fe^+ irradiation at RT increased over four frames, or about 0.13 s. This time is many orders of magnitude longer than expected for a process of cascade collapse, and suggests that loop production involves local point-defect diffusion over distances comparable with the cascade size. This is consistent with recent Monte Carlo simulations of defect clustering within cascade regions in Fe [11]. Data for the 500 °C experiment has not yet been analysed in detail.

Loop motion was induced by the ion beam and the electron beam alone. The phenomenon was observed in all materials, and at both 300 °C and RT, but was particularly pronounced in UHP iron at 300 °C. The motion took the form of sudden one-dimensional jumps of the loop from one position to another, sometimes over distances of more than 10 nm and so has been termed "hopping". The motion usually took place between successive 1/30 s video frames, implying a velocity in excess of 10^3 nm s^{-1}, and so could easily be distinguished from specimen drift. Fig. 3 shows measurements of the position of a loop in UHP Fe as a function of time under 200 keV electron irradiation at 300 °C. This loop had been produced during 150 keV Fe^+ irradiation to a dose of 10^{18} m^{-2}. The direction of hopping was always parallel to the projection of a <111> direction. No instances were found of loops hopping in <100> directions. This is consistent with the hopping loops all having 1/2<111> Burgers vectors. Hopping was not observed at 500 °C, when nearly all loops had <100> Burgers vectors, see below.

Loss of loops by glide to the surface or other mechanisms was seen frequently in the dynamic experiments at both 300 °C and RT, and confirmed directly that the number of loops remaining at the end of the irradiation was often far less than the total number produced during irradiation. In Fe the number of loops retained was strongly dependent on the foil orientation. In orientations

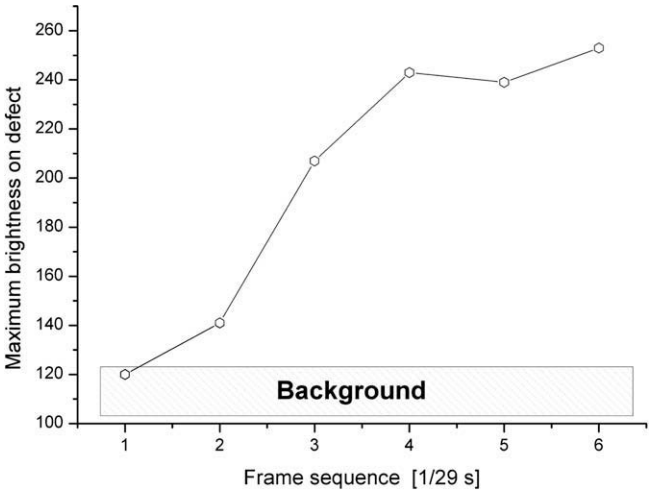

Fig. 2. Appearance of a new loop in Fe–8%Cr during 150 keV Fe^+ irradiation at RT over several frames of a video recording. Shown is the maximum contrast of the loop in successive video frames. In this case the contrast reached a maximum after five frames. Each frame is equal to 1/29 s.

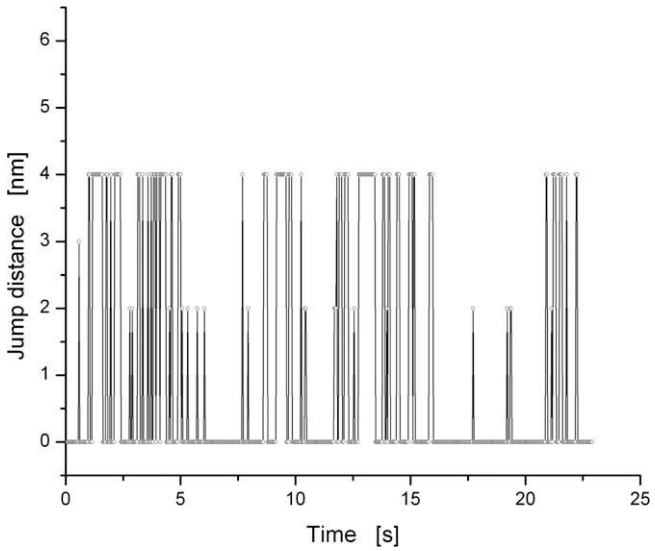

Fig. 3. One-dimensional hopping of an 1/2<111> loop in UHP Fe under 200 keV electron irradiation at 300 °C. The loop had been produced during 150 keV Fe^+ irradiation to a dose of 10^{18} m^{-2}. The loop hopped between four different positions, spending most of its time at the extremes. Its position was measured to the nearest nanometer.

such as (111) the defect yield (i.e. the number of loops present after irradiation relative to the dose) was much lower than in orientations such as (110). The effect is illustrated in Fig. 4, which shows defect yields (measured at a dose of 5×10^{17} m^{-2} in RT experiments) in pure Fe and Fe–11%Cr at different foil orientations. Although the irradiation conditions were different (100 keV Fe^+ ions in the former case, and 30 keV Ga^+ ions in the latter) the defect yields near (110) are comparable. Near (111) however the yield in Fe–11%Cr is nearly two orders of magnitude higher than in Fe. This has a ready explanation if we accept that the effect of Cr is to reduce the mobilities of 1/2<111> loops, so they are less likely to glide to the surface [4]. In a (111) foil of pure Fe, mobile 1/2<111> loops of all four variants are lost to the surface by glide and few are retained in the foil. In a (110) foil however two of the 1/2<111> variants have Burgers vectors in the foil plane, and so cannot be lost by glide. In Fe–Cr alloys however some loops are retained even though their Burgers vectors point towards the surface. Detailed loop counting in dynamic experiments suggested that the initial production of loops did not depend systematically on the alloy composition, but that the effect of Cr on reducing loop mobilities is the main cause of differences in damage development between pure Fe and Fe–Cr alloys [4].

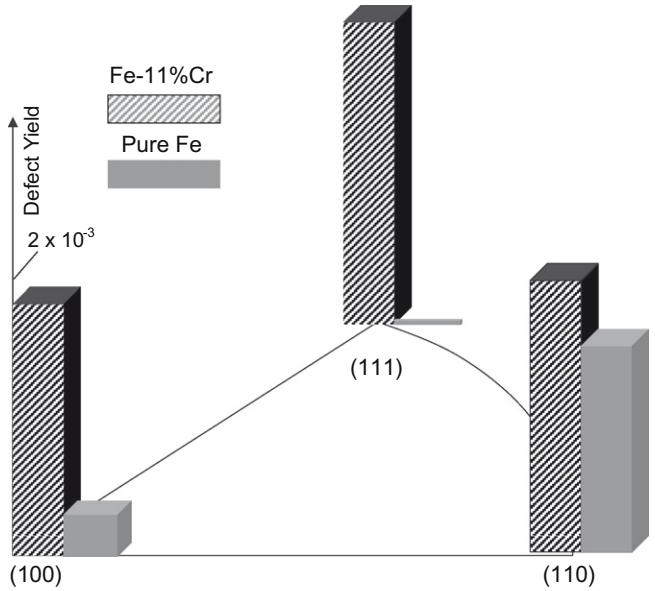

Fig. 4. Relative values of the defect yield in pure Fe (irradiated with 100 keV Fe^+ ions at RT) and Fe–11%Cr (irradiated with 30 keV Ga^+ ions at RT). Despite the different irradiation conditions, the defect yields are comparable in (110) foils. However the yield depends strongly on foil orientation in pure Fe, but not in Fe–11%Cr. Data for pure Fe in the (110) orientation is taken from Ref. [12].

The mechanism by which loop mobility is reduced in the Fe–Cr alloys is still not entirely clear. This reduction cannot be attributed to pinning by resolvable precipitates since none were present. Terentyev et al. [13] have shown that a reduction in mobility of self-interstitial clusters in Fe–Cr alloys relative to pure Fe may be caused by a long-range, attractive interaction between Cr atoms and crowdions. Simulations have not yet been made for the interaction between Cr atoms and larger interstitial loops or vacancy clusters, but a similar effect is plausible.

3.3. Damage development at higher doses

At doses greater than about 2×10^{18} ions m^{-2} (about 1 dpa) complex microstructures started to develop in regions of foils thicker than about 60 nm. A comparison of the microstructures seen at high doses in UHP Fe and Fe–8%Cr is shown in Fig. 5. The microstructures at RT and 300 °C showed strong similarities in both materials, although the characteristic features developed earlier and on a coarser scale at 300 °C than at RT, and in UHP Fe than in Fe–8%Cr. First strings of several loops formed, all with the same 1/2<111> Burgers vectors, seeming to involve cooperative alignment and interaction of smaller loops. The exact mechanism by which this occurred is still unclear. Loop strings in UHP Fe irradiated at RT are seen clearly in panel (a) of Fig. 5. In this case the microstructure did not develop further by the highest dose reached in this experiment. However, in other cases of 300 °C or RT irradiations the strings developed into resolvable loops, as seen in panels (b) and (d) of Fig. 5.

In UHP Fe irradiated at 300 °C large finger-shaped loops developed by the growth and coalescence of smaller loops, see panel (c) of Fig. 5. The process of loop growth and coalescence is shown in Fig. 6, which consists of four frames captured from a video recording over a dose range from about 1 to 1.5×10^{19} ions m^{-2} (6–10 dpa). Contrast analyses showed that these loops had 1/2<111> Burgers vectors, that they were not of pure edge character but had large shear components, and that they were of interstitial nature (see below). Bright spots with contrast which gradually faded were often associated with loop perimeters. These may be small loops which are being assimilated onto the dislocation line, causing climb. In this material very small (1–2 nm) voids were seen at the highest irradiation dose of 2×10^{19} m^{-2} (~13 dpa).

Damage evolved quite differently at 500 °C compared with lower temperatures. In UHP Fe prismatic loops with **b** = <100> and of edge character nucleated and grew by climb and coalescence. By a dose of 10^{19} ions m^{-2} (~6.5 dpa) they reached sizes of several hundred nanometers and formed fairly regular arrays (see Figs. 5e and 7(a) and (b)). These micrographs were taken using a diffraction vector **g** = 110 at a foil orientation close to (001) and the two sets of near edge-on loops with **b** = [100] and [010] are visible as orthogonal lines or pairs of parallel lines. A third set of loops with **b** = [001] which lie in the foil plane and so have **g.b** = 0 are visible in Fig. 7(a) and (b) in **g.b** $\times$**u** contrast [8], often lying within cages formed by sets of edge-on loops. Loops with **b** = [001] were seen to glide out of the foil when they reached large sizes. No loops with **b** = 1/2<111> were found.

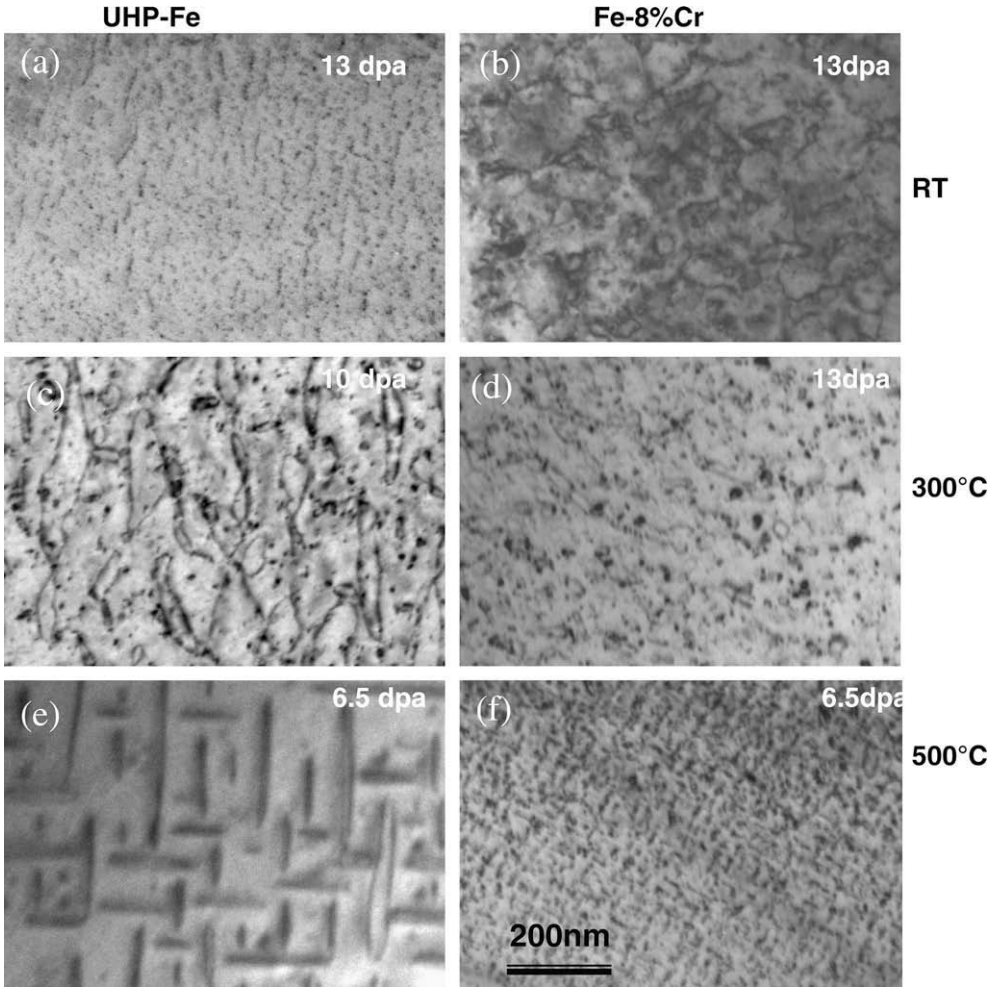

Fig. 5. Comparison of high dose damage structures in UHP Fe and Fe–8%Cr at different irradiation temperatures, as indicated. See the text for details. All are bright-field kinematical images taken with **g** = 110.

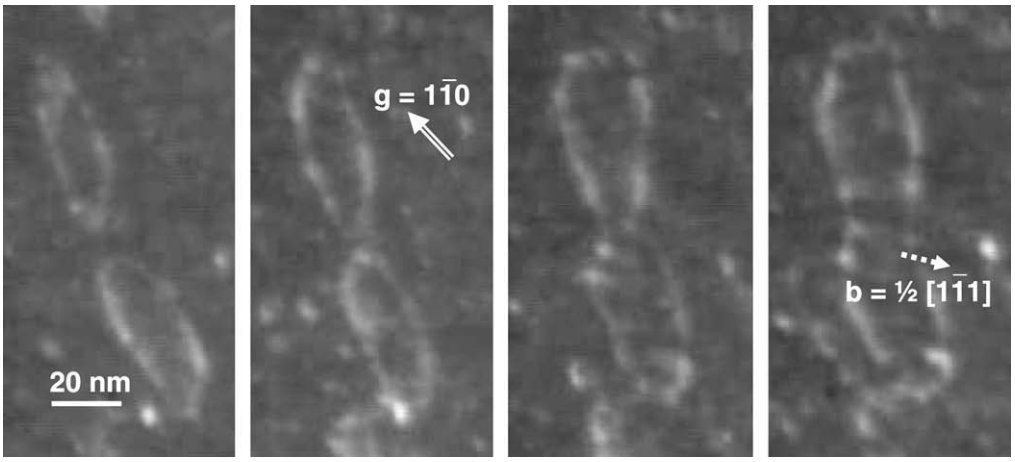

Fig. 6. Growth and coalescence of large 1/2<1 1 1> loop in UHP Fe under irradiation at 300 °C with 150 keV Fe^+ ions, covering a dose range from 10^{19} to 1.5×10^{19} ions m^{-2} (about 6–10 dpa). These are weak-beam images taken in 1$\bar{1}$0. The projection of the Burgers vector of the loops is shown.

The nature of the large loops produced in pure Fe at both 300 °C and 500 °C was established from their inside–outside contrast behavior. This is illustrated for the case of <1 0 0> edge loops produced at 500 °C in Fig. 8. These micrographs were obtained by first tilting the foil about 15° away from the [0 0 1] pole along a 110 Kikuchi band. Micrographs were then recorded under weak-beam conditions using **g** = ±110 with positive deviation parameter s_g, keeping the magnitude $|s_g|$ constant. Two sets of steeply inclined <1 0 0> loops are imaged. The set of loops marked A shows inside contrast in Fig. 8(a) and outside contrast in Fig. 8(b). The set of

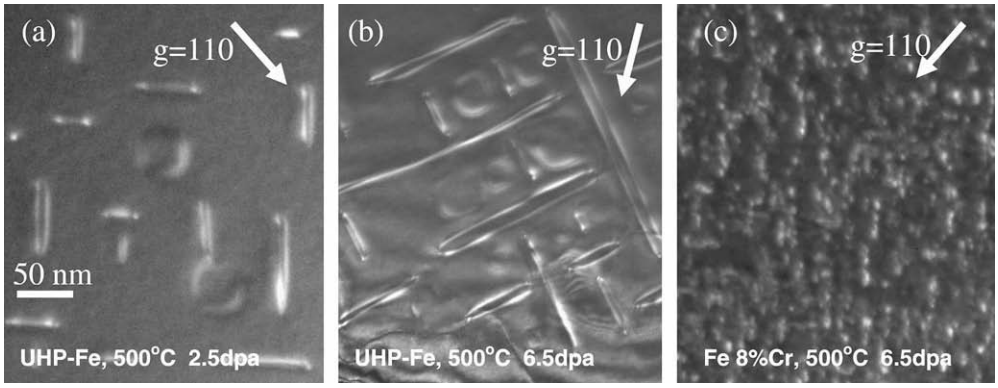

Fig. 7. Details of the damage structures in UHP Fe and Fe–8%Cr at 500 °C. In both cases the microstructure is dominated by edge <100> loops. All are weak-beam images taken with **g** = 110. See text for details.

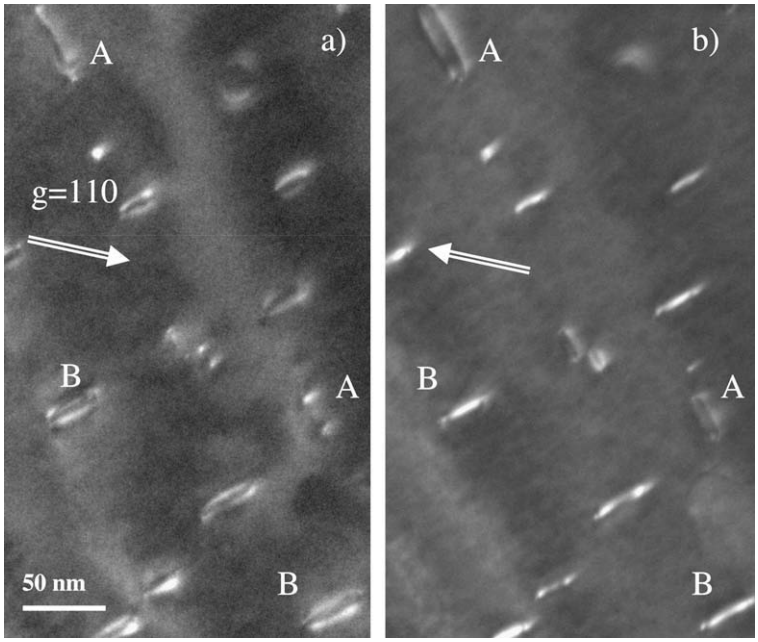

Fig. 8. Inside–outside contrast behavior of edge <100> loops in UHP Fe irradiated at 500 °C to 3×10^{19} ions m^{-2}. The contrast changes are consistent with an interstitial nature.

loops B shows the opposite behavior. Since both sets of loops were edge-on at [001], the direction of tilt along the 110 Kikuchi band relative to this pole was sufficient to establish the sense of inclination of each set of loops at the imaging orientation. The **g**-vectors were placed on the micrographs, taking care to include the 180° inversion between diffraction pattern and image caused by the objective lens. The inside–outside contrast is consistent with both sets of loops having interstitial nature. The nature of the non-edge

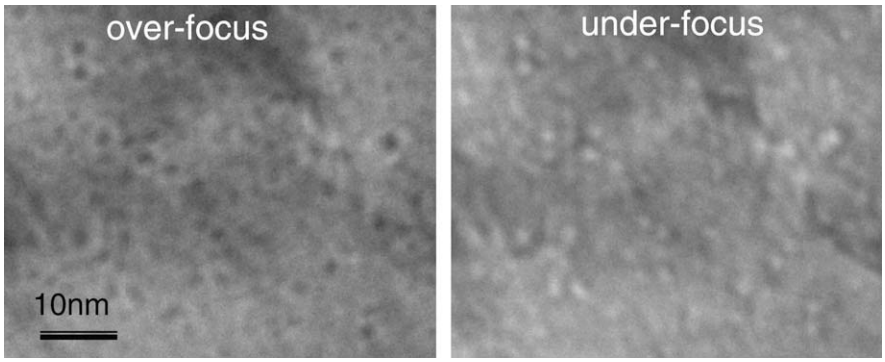

Fig. 9. Probable voids in Fe–8%Cr irradiated with 150 keV Fe^+ ions at 500 °C to a dose of 10^{19} m^{-2} (about 6.5 dpa).

1/2<111> loops produced at 300 °C was determined by a similar but more involved procedure. These were also found to be interstitial (see Refs. [4] and [8] for further details of the method).

In Fe–8%Cr irradiated at 500 °C, loops with **b** = <100> were also found with few if any loops with **b** = 1/2<111>. However the damage was on a much finer scale than in pure Fe, with a much higher loop number density and maximum loop sizes of a few tens of nanometers (see Figs. 5f and 7(c)). In this material small voids were also identified at the highest dose (Fig. 9).

Our experimental observation that only loops with **b** = <100> are produced in Fe and Fe–Cr alloys at 500 °C, whereas loops with both **b** = <100> and 1/2<111> occur at temperatures $\leqslant$300 °C, is consistent with recent theoretical work by Dudarev et al. [14]. These authors argued that a temperature dependence of the anisotropic elastic free energies provides a fundamental explanation why <100> loops become increasingly favourable at temperatures >300 °C.

4. Conclusions

Thin foils of Fe–0–18%Cr alloys were irradiated with 100–150 keV Fe^+ and Xe^+ ions at RT, 300 °C and 500 °C. Dynamic TEM observations followed the evolution of damage over doses $\leqslant 2 \times 10^{19}$ ions m^{-2} ($\sim$13 dpa). The main results were:

- Small 2–4 nm dislocation loops first appeared at doses of about 10^{16} and 10^{17} ions m^{-2}, much higher than in many other materials. In irradiations at RT and 300 °C loops with both <100> and 1/2<111> Burgers vectors were present, whilst at 500ºC only loops with **b** = <100> were seen.
- The contrast of new loops often developed over time intervals as long as 0.2 s, many orders of magnitude longer than expected for a process of cascade collapse.
- At 300 °C and RT, loop hopping and loss of 1/2<111> loops to the surface was induced by both ion irradiation and the electron beam alone.
- In Fe the number of loops retained was strongly dependent on the foil orientation; less loop loss occurred in Fe–Cr alloys. This is attributed to the effect of Cr in reducing loop mobilities.
- At doses greater than about 2×10^{18} ions m^{-2}, complex microstructures developed in thicker regions of foils, but these microstructures were quite different at 500 °C than at lower irradiation temperatures. In UHP Fe irradiated at 300 °C the damage took the form of prismatic interstitial loops with **b** = 1/2<111>. Large finger-shaped loops developed by the growth and coalescence of smaller loops. At 500 °C in the same material large edge loops with **b** = <100> developed.
- Similar damage structures developed at higher doses in Fe–8%Cr at each irradiation temperature, although on a finer scale than in pure Fe. At RT and 300 °C most loops had **b** = 1/2<111>; at 500 °C almost all had **b** = <100>.

Acknowledgements

The IVEM-Tandem Facility (within the Electron Microscopy Center at ANL) is supported by the US DOE Office of Science and operated under contract No. DE-AC02-06CH11357 by UChicago Argonne, LLC. We thank Dr A. Liu and P. Baldo of Argonne National Lab for their help in using this facility. Part of this work was funded by the UKAEA, Culham Science Centre. We are grateful to Dr S. L. Dudarev and Dr C. A. English for helpful discussions.

References

[1] D.S. Gelles, J. Nucl. Mater. 233–237 A (1996) 293.
[2] R.L. Klueh, D.R. Harries, High Chromium Ferritic and Martensitic Steels for Nuclear Applications, American Society for Testing and Materials, West Conshohocken, PA, USA, 2001.
[3] K. Ehrlich, Fus. Eng. Des. 56&57 (2001) 71.
[4] Z. Yao, M. Hernández-Mayoral, M.L. Jenkins, M.A. Kirk, Phil. Mag. 88 (2008) 2851.
[5] M. Hernández-Mayoral, Z. Yao, M.L. Jenkins, M.A. Kirk, Phil. Mag. 88 (2008) 2881.
[6] C.W. Allen, L.L. Funk, E.A. Ryan, Mat. Res. Soc. Symp. Proc. 396 (1996) 641.
[7] J. F. Ziegler, J. P. Biersack, The Stopping and Range of Ions in Matter, SRIM-2003, ©1998, 1999 by IB77M co.
[8] M. L. Jenkins, M. A. Kirk, Characterisation of Radiation Damage by Transmission Electron Microscopy, in: B. Cantor, M. J. Goringe (Eds.), Institute of Physics Series in Microscopy in Materials Science, 2001, ISBN: 0 7503 0748 X (hbk).
[9] M.A. Kirk, I.M. Robertson, W.E. King, W.E. Ryan, A. Philippedes, Mater. Res. Soc. Proc. 41 (1985) 315.
[10] M.L. Jenkins, C.A. English, B.L. Eyre, Phil. Mag. 38 (1978) 97.
[11] M. Gilbert, S.L. Dudarev, P. Derlet, D.G. Pettifor, J. Phys.: Condens. Mat. 20 (2008) 345214.
[12] M.A. Kirk, I.M. Robertson, M.L. Jenkins, C.A. English, T.J. Black, J.S. Vetrano, J. Nucl. Mater. 149 (1987) 21.
[13] D. Terentyev, L. Malerba, A.V. Barashev, Phil. Mag. Lett. 85 (2005) 587.
[14] S.L. Dudarev, R. Bullough, P.M. Derlet, Phys. Rev. Lett. 100 (2008) 135503.